Characterization of Phosphine Complexes of Technetium(III) as Transport Substrates of the Multidrug Resistance P-Glycoprotein and Functional Markers of P-Glycoprotein at the Blood−Brain Barrier†

Gary D. Luker, Vallabhaneni V. Rao, Carolyn L. Crankshaw, Julie Dahlheimer, and David Piwnica-Worms*

Laboratory of Molecular Radiopharmacology, Departments of Radiology and Molecular Biology and Pharmacology, Washington University Medical School, St. Louis, Missouri 63110

Received August 5, 1997⊗

ABSTRACT: The multidrug resistance (*MDR1*) P-glycoprotein functions as a broad specificity efflux transporter of structurally diverse natural product and xenobiotic compounds. P-glycoprotein also is an important component of the functional blood−brain barrier. To enable further studies of function and modulation of *MDR1* P-glycoprotein *in vitro* and *in vivo*, two novel phosphine technetium(III) complexes were designed and characterized: *trans*-[2,2′-(1,2-ethanediyldiimino)bis(1,5-methoxy-5-methyl-4-oxo-hexenyl)]bis[methylbis(3-methoxy-1-propyl)phosphine]Tc(III) (Tc−Q58) and *trans*-[5,5′-(1,2-ethanediyl diimino)bis(2-ethoxy-2-methyl-3-oxo-4-pentenyl)]bis[dimethyl(3-methoxy-1-propyl)phosphine)]Tc(III) (Tc−Q63). In human drug-sensitive KB 3-1 cells and multidrug-resistant KB 8-5 and 8-5-11 derivative cell lines, expressing nonimmunodetectable, low, and high levels of *MDR1* P-glycoprotein, respectively, accumulation of Tc−Q58 and Tc−Q63 was inverse to expression of the transporter. Differences between drug-sensitive and multidrug-resistant cells, while detectable at picomolar concentrations of each radiopharmaceutical, were independent of tracer concentration. Ratios of tracer accumulation in KB 3-1 and 8-5 cells were 62.3 and 48.1 for Tc−Q58 and Tc−Q63, respectively. Cell contents of Tc−Q58 and Tc−Q63 were enhanced up to 60-fold in MDR cells by known modulators of *MDR1* P-glycoprotein, while drugs not in the multidrug-resistant phenotype had no effect on their accumulation. In KB 8-5 cells, potency of modulators was GF120918 ≫ cyclosporin A > verapamil. Accumulation of Tc−Q58 and Tc−Q63 in Sf9 insect cells infected with a recombinant baculovirus containing human *MDR1* P-glycoprotein was reduced in a GF120918-reversible manner ($EC_{50} \leq 70$ nM) compared with cells infected with a wild-type baculovirus. By contrast, cell contents of Tc−Q58 or Tc−Q63 in Sf9 cells expressing the homologous *MDR3* P-glycoprotein did not differ from wild-type virus. Demonstrating molecular targeting of these complexes *in vivo*, distribution and retention of Tc−Q58 in brain tissue of FVB mice treated with a saturating dose of GF120918 and mice deficient in the *mdr1a* gene [*mdr1a* (−/−)] were enhanced 180% and 520% over control, respectively. Exploiting the gamma-emission spectrum of ^{99m}Tc, increased uptake of Tc−Q58 in brain tissue of *mdr1a* (−/−) mice was readily detected noninvasively by scintigraphic imaging. Thus, both Tc−Q58 and Tc−Q63 are demonstrated to be substrates for transport by *MDR1* P-glycoprotein, broadening the specificity of this transporter to include phosphine-containing metal complexes. As shown with Tc−Q58, these Q complexes can be used to detect transport activity and modulation of *MDR1* P-glycoprotein *in vitro* and to directly monitor the functional status of P-glycoprotein at the blood−brain barrier *in vivo*.

Resistance of malignant tumors to chemotherapy is a major cause of treatment failure (*1*−*3*). Multidrug resistance (MDR[1]) conferred by overexpression of *MDR1* P-glycoprotein is one of the best characterized forms of transporter-mediated resistance (*4*, *5*) and remains an attractive target for improving anticancer therapies. *MDR1* P-glycoprotein is an ≈170 kDa transmembrane protein that appears to function as an energy-dependent efflux pump for reducing intracellular concentrations of chemotherapeutic agents. Although substrates for *MDR1* P-glycoprotein are structurally and functionally diverse, these compounds typically are hydrophobic and cationic at physiological pH (*3*, *6*). In a variety of tumors, expression of *MDR1* P-glycoprotein and related members of the ATP-binding cassette transporter family ([e.g., multidrug-resistance associated protein (MRP) (*7*)] is an important prognostic indicator at the time of diagnosis, while increased levels of P-glycoprotein are found in a high proportion of relapsing cancers (*8*−*12*).

In addition to expression in tumors, *MDR1* P-glycoprotein normally is present in many different tissues, including intestinal epithelium, kidney, liver, adrenal, and endothelial cells in capillaries at the blood−brain and blood−testis barriers (*13*). Although the function of *MDR1* P-glycoprotein in normal physiology remains under active investigation, the protein appears to limit entry of a wide variety of hydrophobic compounds into the central nervous system (*14*). Mice

† This work was supported by the U.S. Department of Energy (ER61885) and a research contract from Mallinckrodt Medical, Inc. G.D.L. is a recipient of a Radiological Society of North America Research Fellowship and a Society of Nuclear Medicine Grant.

* Address correspondence to this author at the Mallinckrodt Institute of Radiology, 510 S. Kingshighway Blvd., St. Louis, MO 63110 [telephone (314) 362-9356; fax (314) 362-0152; e-mail piwnica-worms@mirlink.wustl.edu].

⊗ Abstract published in *Advance ACS Abstracts,* November 1, 1997.

[1] Abbreviations: AUC, area-under-the-curve; MDR, multidrug resistance; MRP, multidrug resistance-associated protein.

S0006-2960(97)01931-4 CCC: $14.00

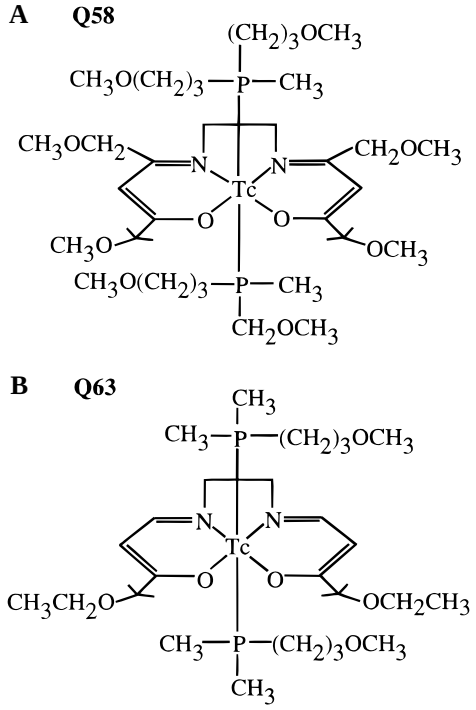

FIGURE 1: Structures of (A) Tc−Q58 and (B) Tc−Q63.

that are genetically deficient in *mdr1a* P-glycoprotein [*mdr1a* (−/−) mice] accumulate 50-fold more ivermectin, a substrate for P-glycoprotein, within brain parenchyma than the parental strain (*14*). Consequently, *mdr1a* (−/−) mice developed a fatal neurotoxicity when treated with this drug. Symptoms of neurotoxicity also have occurred in humans during phase I clinical trials with potent new modulators of *MDR1* P-glycoprotein. For example, severe ataxia was the dose-limiting toxicity in patients receiving PSC 833, a second-generation modulator, in combination with etoposide (*15*). Thus, drug-transporting P-glycoproteins (*MDR1* in humans and *mdr1a* in mice) are important components of the blood−brain barrier. The ability to directly monitor function of P-glycoprotein at the blood−brain barrier would be a significant advance for studies in neurobiology and cancer chemotherapy.

$N_2O_2P_2$−technetium(III) complexes (Q complexes) are a general class of nonreducible, mixed ligand technetium (^{99m}Tc) coordination compounds suitable for scintigraphic imaging (*16*, *17*). These complexes are stable monovalent cations in which two hydrophobic phosphine substituents and a planar Schiff base ligand fill the coordination sphere of the core technetium(III) metal (Figure 1) (*16*, *18*). We postulated that selected members of this class of nonreducible Tc(III) cations could be designed to simulate known amphipathic substrates of *MDR1* P-glycoprotein. Thus, we recently synthesized and functionally screened 38 different $N_2O_2P_2$−technetium(III) complexes as potential transport substrates for P-glycoprotein (*18*). On the basis of systematic modifications of the general ligand structure, we identified two compounds, *trans*-[2,2′-(1,2-ethanediyldiimino)bis(1,5-methoxy-5-methyl-4-oxo-hexenyl)]bis[methylbis(3-methoxy-1-propyl)phosphine]Tc(III) (Tc−Q58) and *trans*-[5,5′-(1,2-ethanediyldiimino)bis(2-ethoxy-2-methyl-3-oxo-4-pentenyl)]bis[dimethyl(3-methoxy-1-propyl)phosphine)]Tc(III) (Tc−Q63), which held promise as radiosubstrates for transport by *MDR1* P-glycoprotein, based on large differences in accumulation between drug-sensitive and multidrug-resistant cells. In the present study, we characterize more completely the biochemical and pharmacological interactions of Tc−Q58 and Tc−Q63 with *MDR1* and *MDR3* P-glycoproteins. In addition, as demonstrated by Tc−Q58, the gamma-emission spectrum of these Q complexes can be exploited for noninvasive imaging of the function and modulation of P-glycoprotein at the blood−brain barrier *in vivo.*

EXPERIMENTAL PROCEDURES

Solutions and Reagents. Stock solutions of verapamil, methotrexate, *cis*-platin (Sigma Chemical Co., St. Louis, MO), and GF120918 (gift of Glaxo-Wellcome, Research Triangle Park, NC) were prepared in dimethyl sulfoxide (DMSO). Final concentration of DMSO in experimental buffers was <1%, which has been found to have no effect on net uptake of Tc complexes in cultured cells (*19*). Cyclosporin A (Novartis-Sandoz Pharmaceuticals) was provided as a Cremephor formulation and added to buffers in the concentrations indicated. All other reagents were obtained from Sigma.

Control solution for transport experiments was a modified Earle's balanced salt solution (MEBSS) containing (mM) 145 Na^+, 5.4 K^+, 1.2 Ca^{2+}, 0.8 Mg^{2+}, 152 Cl^-, 0.8 $H_2PO_4^-$, 0.8 SO_4^{2-}, 5.6 dextrose, 4.0 HEPES, and 1% bovine calf serum (v/v), pH 7.4 ± 0.05. A 130 mM K^+/20 mM Cl^- solution was made by equimolar substitution of potassium methanesulfonate for NaCl as described (*20*).

Cell Culture. Monolayers of human epidermoid carcinoma KB 3-1 cells and the colchicine-selected KB 8-5 and KB 8-5-11 derivative cell lines were grown as previously described (*21*, *22*). Briefly, cells were plated in 100-mm Petri dishes containing seven 25-mm glass coverslips on the bottom and grown to confluence in DMEM (Gibco, Grand Island, NY) supplemented with L-glutamine (1%), penicillin/streptomycin (0.1%), and heat-inactivated fetal calf serum (10%) in the presence of 0, 10, and 100 ng/mL colchicine, respectively.

Wild-type baculovirus (*Autographa californica*) was obtained from Invitrogen (San Diego, CA), and recombinant baculoviruses containing human *MDR1* and *MDR3* were the generous gift of James Croop, Dana Farber Cancer Institute, Boston, MA (*23*). The permissive host insect cell line, *Spodoptera frugiperda* (Sf9), was grown as previously described (*24*). Sf9 cells were infected with wild-type or recombinant baculovirus at 5 PFU per cell and harvested using procedures described previously (*25*, *26*). For transport assays, virus-infected Sf9 cells were cultured in 100 mm Petri dishes containing seven glass coverslips with $\approx 1 \times 10^7$ cells per dish. Experiments were performed at 44−48 h following infection, the optimal time for cell transport studies as we described previously (*24*).

Preparation of Tc Complexes. Synthesis of the radiolabeled compound ^{99m}Tc−Sestamibi was performed with a one-step kit formulation (Cardiolite, kindly provided by E. I. DuPont, Medical Products Division, Billerica, MA) (*27*). Synthesis of the Schiff base and phosphine ligands as well as the ^{99m}Tc−Q58 and ^{99m}Tc−Q63 complexes (Mallinckrodt, Inc., St. Louis, MO) was performed as previously described (*16*−*18*). Schiff base and phosphine ligands were characterized by ^{1}H and ^{13}C NMR, infrared (IR), and elemental analysis to validate structure and purity. For synthesis of

the radiolabeled ^{99m}Tc−Q complexes, a standard two-step procedure was employed: In the first step, $^{99m}TcO_4^-$ from a commercial Mo/Tc generator was added to a vial containing the desired Schiff base, $SnCl_2$, and NaOH and heated to yield the ^{99m}Tc(V) intermediate. In the second step, phosphine was added to the warm ^{99m}Tc(V) preparation, and the resulting solution heated to yield the desired ^{99m}Tc(III)−Q complex. Separation of the radiolabeled complex from impurities and reaction reagents was performed by reversed-phase HPLC purification with an acetonitrile/KH_2PO_4 gradient. The HPLC eluent was then removed from the desired complex by diluting the collected HPLC fraction with water, loading it onto a prewet C_{18} Sep-Pak, and eluting the product with 80:20 ethanol/saline. Product eluate was diluted with normal saline to obtain an ethanol concentration of 10%. Quality control effected by reversed-phase HPLC (same conditions as above) showed >90% radiochemical purities. Final structures of ^{99m}Tc−Q58 and ^{99m}Tc−Q63 are shown in Figure 1. Final concentration of the ethanol vehicle in experimental buffers was <0.5%. This concentration of ethanol has been shown previously to have no effect on transport kinetics of a ^{99m}Tc complex in cultured cells (*28*).

Cell Transport Studies. Coverslips with confluent cells were used for studies of cell transport and kinetics as previously described (*21*). In summary, cells were removed from culture media and pre-equilibrated for 15−30 s in control buffer. Accumulation experiments were initiated by immersing coverslips in 60-mm glass Pyrex dishes containing 4 mL of loading solution consisting of MEBSS with 0.1−0.6 nM [Tc complex] (5−9 pmol/mCi; 1.5−2 μCi/mL). Coverslips with cells were removed at various times, rinsed three times in 25 mL of ice-cold isotope-free solution for 8 s each to clear extracellular spaces, and placed in 35-mm plastic Petri dishes. Cells were extracted in 1% sodium dodecyl sulfate with 10 mM sodium borate before protein assay according to the method of Lowry (*29*) (KB cells) or by BCA analysis (Pierce Chemical) (Sf9 cells), using bovine serum albumin as the protein standard. Aliquots of the loading buffer and stock solutions also were obtained for standardizing cellular data with extracellular concentration of each Tc complex. Cell extracts, stock solutions, and extracellular buffer samples were assayed for gamma activity in a well-type sodium iodide gamma counter (Cobra II, Packard, Meridan, CT.). The absolute concentration of total Tc complex in solution was determined from the activity of stock solutions and specific activity of technetium, on the basis of equations of Mo/Tc generator equilibrium (*30*). Data are reported as fmol of Tc complex (mg of protein)$^{-1}$ (nM$_0$)$^{-1}$ as previously described, with (nM$_0$)$^{-1}$ representing total concentration of Tc complex in the extracellular buffer (*28*).

Western Blots. P-glycoprotein was detected in crude, enriched membrane preparations from KB cell lines, Sf9 cells, and infected Sf9 cells, using Western blotting with monoclonal antibody C219 (Signet Corp., Dedham, MA). Immune complexes were identified with goat anti-mouse antibody coupled to alkaline phosphatase as previously described (*24*) or with sheep anti-mouse antibody (1:2000 dilution) coupled to horseradish peroxidase using the ECL Western blotting detection system (Amersham Life Sciences, Arlington Heights, IL).

Biodistribution Studies. Vertebral animal procedures were approved by the appropriate institutional review committees. Distribution of ^{99m}Tc−Q58 in the blood and brain tissues of parental strain FVB mice (FVB/NTacfBR) and FVB *mdr1a* (−/−) gene knockout mice (FVB/TacfBR-[KO]*mdr1a*N7) (Taconic, Germantown, NY) was determined as previously described (*31*). For experiments using GF120918 in parental FVB mice, the drug was prepared in 0.5% hydroxypropylmethylcellulose/1% Tween-80/dH_2O vehicle and administered by oral gavage (250 mg/kg of body weight) 4 h prior to injection of ^{99m}Tc−Q58; control animals for these experiments received vehicle only. Approximately 4 h after oral administration of modulator, peak serum levels of 500−600 ng/mL are achieved (unpublished data and ref *32*), a concentration of drug shown to be saturating for inhibition of *MDR1* P-glycoprotein-mediated transport activity *in vitro*. ^{99m}Tc−Q58 was diluted in 90:10 saline/ethanol for a final concentration of 20 μCi/mL. Mice were anesthetized by metafane inhalation and injected with 2 μCi (5−9 pmol/mCi) of radiotracer via bolus injection through a tail vein. Animals were sacrificed by cervical dislocation at 5, 15, 30, 60, and 120 min postinjection ($n = 2-4$ each). Blood samples were obtained by cardiac puncture, and brain tissue was harvested rapidly. Gamma activity in organ samples was counted for 1 min, or until two standard deviations of sampling were <0.5%. Radio-HPLC analysis of tissue extracts confirmed recovery of nearly 95% of parental complex (M. Marmion, unpublished data). Data are expressed as percent of injected dose per gram of tissue [(tissue μCi) (injected μCi)$^{-1}$ (g tissue)$^{-1}$ × 100].

Imaging Studies. FVB and FVB *mdr1a* (−/−) mice were anesthetized with a ketamine (75 mg/kg)/medetomidine (1 mg/kg) cocktail. ^{99m}Tc−Q58 (125 μCi in 50 μl of 10% EtOH/saline) was injected via a tail vein into mice positioned under a gamma scintillation camera (Siemens Basicam, Siemens Medical Systems, Iselin, NJ; 5 mm pinhole collimator; 20% energy window centered over 140 keV photopeak of ^{99m}Tc). Sequential posterior images of mice were collected at one frame/minute for 20−60 min with a 128 × 128 matrix and corrected for radioactive decay. Brain accumulation of ^{99m}Tc−Q58 was analyzed by manually drawing regions of interest over the brain parenchyma and subtracting background radioactivity determined from a region of interest placed adjacent to the head of each mouse. No corrections were made for scatter or attenuation. In pseudo-gray-scale images, liver was masked with a saturation cutoff filter to highlight contrast differences in brain.

Analysis. All data points for transport assays were determined from preparations obtained from the same culture. EC_{50} values (half-maximal effective concentration of drug) for modulators were estimated by computer fit (Sigma Plot, Jandel Scientific) of concentration−effect curves of Tc complex transport inhibition using the sigmoid equation

$$C = \{(C_{max} - C_{min})/[1 + (D/EC_{50})^{\gamma}]\} + C_{min} \quad (1)$$

where C is cell content of Tc complex, C_{max} is maximum cell content of Tc complex, C_{min} is minimum cell content of Tc complex, γ is the slope, D is concentration of MDR modulator, and EC_{50} represents the half-maximal effective concentration (*33*).

From biodistribution time−activity curves, area-under-the-curve was calculated using trapezoidal integration (KaleidoGraph, Synergy Software) and reported as tissue μCi (injected μCi)$^{-1}$ (g of tissue)$^{-1}$ × 100·minute. Data are

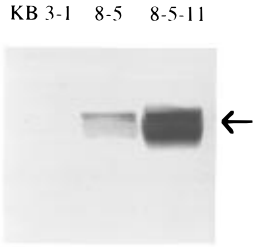

FIGURE 2: Expression of P-glycoprotein in human KB epidermoid carcinoma cells as determined by Western blot of plasma membrane preparations with mAb C219. The arrow identifies 170 kDa.

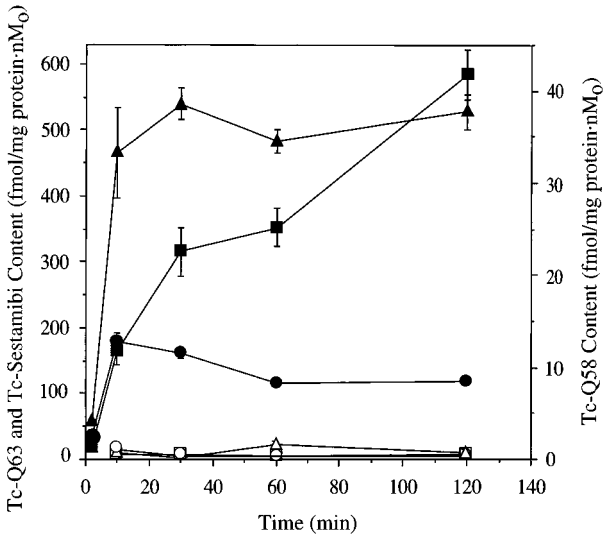

FIGURE 3: Kinetics of Tc complex accumulation in KB cells for Tc−Q58 (KB 3-1, ▲; KB 8-5, △), Tc−Q63 (KB 3-1, ■; KB 8-5, □), and Tc−Sestamibi (KB 3-1, ●; KB 8-5, ○). Cells were incubated in buffer for the indicated times. Note different scales on the *y*-axis for cell-associated uptake of Tc−Q63 and Tc−Sestamibi (left) and Tc−Q58 (right). Each point represents the mean of four determinations; bars represent ± SEM when larger than the symbol.

reported as mean ± SEM. Pairs were compared by Student's *t* test. Values of $p \leq 0.05$ were considered significant.

RESULTS

Validation of Tc−Q58 and Tc−Q63 as Model Substrates for MDR1 P-Glycoprotein

Cell Transport Kinetics in KB Cells. To validate Tc−Q58 and Tc−Q63 as probes of *MDR1* P-glycoprotein transport activity, net tracer uptake and reversal experiments initially were performed in cell lines that express various levels of *MDR1* P-glycoprotein. Human KB 3-1 epidermoid carcinoma cells and the colchicine-selected KB 8-5 and KB 8-5-11 derivative cell lines express nonimmunodetectable, low, and high levels of *MDR1* P-glycoprotein, respectively (Figure 2). Tc−Sestamibi, a radiopharmaceutical previously established as a substrate for transport by P-glycoprotein (*21*), was used as a positive control in these experiments. When exposed to tracer quantities of Tc−Q58, KB 3-1 and 8-5 cells in monolayer culture accumulated the radiolabel to different plateaus within 10 min (Figure 3). Similarly, content of Tc−Sestamibi in these two KB cell lines reached different steady states within 10 min. Steady-state values for Tc−Q58 in KB 3-1 and 8-5 cells were 58.0 ± 4.2 and 0.93 ± 0.17 fmol (mg of protein)$^{-1}$ (nM$_0$)$^{-1}$ ($n = 12$; $p < 0.001$), respectively, compared with 187 ± 12 and 3.8 ± 0.2 fmol (mg of protein)$^{-1}$ (nM$_0$)$^{-1}$ ($n = 8$; $p < 0.001$) for Tc−Sestamibi. By contrast, while accumulation of Tc−Q63 in KB 8-5 cells also reached a plateau within 10 min [6.6 ± 0.6 fmol (mg of protein)$^{-1}$ (nM$_0$)$^{-1}$ ($n = 8$)], net uptake of Tc−Q63 in KB 3-1 cells after 30 min of incubation was 316 ± 37 fmol (mg of protein)$^{-1}$ (nM$_0$)$^{-1}$ ($p < 0.005$) and continued to increase through 2 h of incubation to 585 ± 38 fmol (mg of protein)$^{-1}$ (nM$_0$)$^{-1}$ ($n = 8$). The ratio of steady-state accumulation of each radiopharmaceutical in KB 3-1 and KB 8-5 cells (or content of Tc−Q63 at 30 min of incubation) was used as a measure of differential detection of functional *MDR1* P-glycoprotein, thereby correcting for differences in absolute cell content of each Tc complex. Ratios of cell accumulation (KB 3-1/KB 8-5 cells) were 62.3, 48.1, and 48.4 for Tc−Q58, Tc−Q63, and Tc−Sestamibi, respectively. These data suggest that detection of functional *MDR1* P-glycoprotein in KB cells using Tc−Q58 and Tc−Q63 is superior or equal to that of Tc−Sestamibi.

To further define the interactions of Q complexes with cells, monolayers of confluent KB 3-1 cells were incubated with tracer amounts of each Tc complex in buffer alone or buffer containing 130 mM K^+/20 mM Cl^- and 1 mg/mL of the potassium ionophore valinomycin. Under these conditions, electrical potentials of the mitochondrial membrane ($\Delta\Psi$) and plasma membrane (E_m) are depolarized toward zero, eliminating the inward driving force for uptake of hydrophobic cations such as the Q complexes (*28*). The residual net accumulation of each radiopharmaceutical under isoelectric membrane potential is one measure of nonspecific adsorption of hydrophobic cationic complexes to lipid compartments in cells (*28, 34*). Prior studies have established that Tc−Sestamibi is a Nernstian probe of membrane potential with minimal adsorptive binding to lipid bilayers (*28*, *35*, *36*). Thus, in the presence of high K^+ and valinomycin, residual uptake of Tc−Sestamibi maps intracellular water space (*28*, *35*). For Tc−Q58, Tc−Q63, and Tc−Sestamibi, net uptake of each complex in KB 3-1 cells (30 min of incubation) under isoelectric membrane potential was 7.3 ± 0.3, 74.5 ± 8.8, and 5.1 ± 0.2 fmol (mg of protein)$^{-1}$ (nM$_0$)$^{-1}$ ($n = 4$ each), respectively. By contrast, in KB 3-1 cells incubated in control buffer, accumulation of Tc−Q58 was much less than predicted by membrane potential as defined by Tc−Sestamibi [58.0 ± 4.2 versus 187 ± 12 fmol (mg of protein)$^{-1}$ (nM$_0$)$^{-1}$]. Reduced uptake of Tc−Q58 in steady state may be due to decreased permeability of this complex across the plasma membrane or transport of Tc−Q58 out of cells by another undetermined transporter. While content of Tc−Q58 in KB 3-1 cells under isoelectric conditions was coincident with accumulation into the intracellular water spaces as defined by Tc−Sestamibi, accumulation of Tc−Q63 in KB 3-1 cells was large and continued to increase throughout a 2-h incubation. Being insensitive to depolarization of $\Delta\Psi$ and E_m, these uptake data functionally suggest that Tc−Q63 is continually incorporated into lipid compartments during incubation with cells.

Pharmacological Analysis in KB Cells. To determine if cell content of Tc−Q58 and Tc−Q63 in KB cells could be increased by inhibition of P-glycoprotein, the effects of several known modulators of *MDR1* P-glycoprotein function were tested over a wide range of concentrations. Cell content of each radiopharmaceutical in cell monolayers was determined after 30 min of incubation with each drug. The 30-min incubation period is within times of steady-state

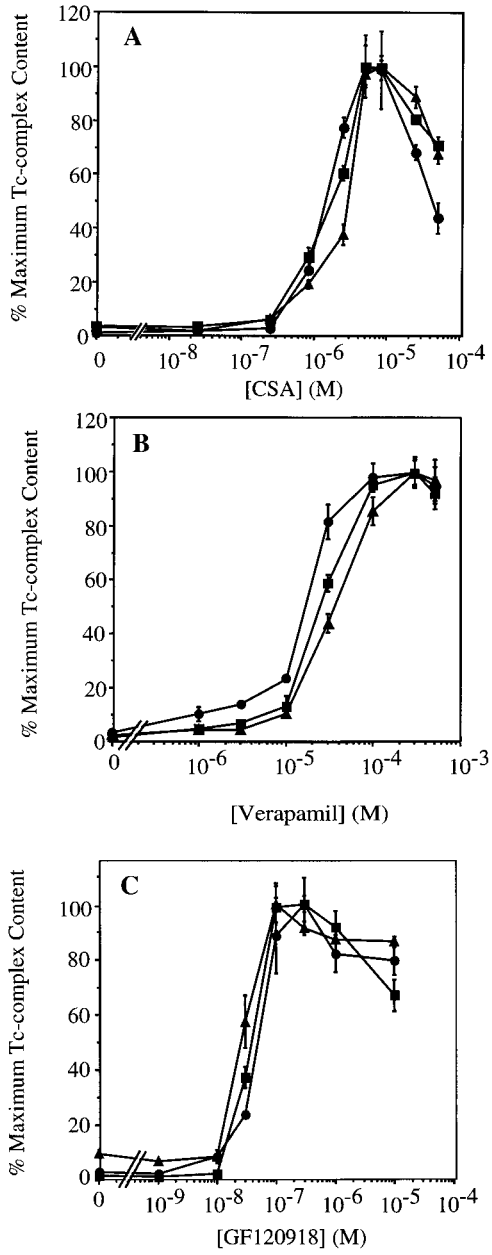

FIGURE 4: Effects of modulators on Tc complex cellular accumulation in cells with low levels of *MDR1* P-glycoprotein. KB 8-5 cells were incubated for 30 min in buffer containing a Tc complex (Tc−Q58, ▲; Tc−Q63, ■; Tc−Sestamibi, ●) and the indicated concentrations of (A) cyclosporin A, (B) verapamil, and (C) GF120918. Percent of maximum cellular content of each Tc complex is plotted. C_{max} values for each complex are shown in Table 1. Each point represents the mean of four determinations; bars represent ± SEM.

accumulation for Tc−Sestamibi and Tc−Q58 in all KB cells and Tc−Q63 in KB 8-5 cells. (Accumulation of Tc−Q63 in KB 3-1 cells was terminated at 30 min to remain contemporaneous with the other two compounds.) As shown in Figure 4, cyclosporin A and verapamil, first-generation modulators of *MDR1* P-glycoprotein, and GF120918, a high-potency, third-generation modulator of P-glycoprotein, were all found to enhance uptake of the Tc complexes in KB 8-5 cells. For all three Tc complexes, the relative rank order of potency of the modulators was GF120918 ≫ cyclosporin A > verapamil (Table 1). The EC_{50} values for GF120918 were approximately 85−100-fold less than those for cyclosporin A for each Tc complex. At the highest concentrations of cyclosporin A, accumulation of each Tc complex rolled below maximal cell content (C_{max}), likely due to toxicity of cyclosporin A, which is known to affect targets in cells other than P-glycoprotein (*37*, *38*). Slightly decreased accumulation of Tc complexes at high concentrations of GF120918 was also seen in KB 8-5 cells, although the effect is much less than with cyclosporin A. EC_{50} values for verapamil in KB 8-5 cells were more variable among the three Tc complexes than the values for cyclosporin A and GF120918, although these differences were not statistically significant. The reversal curve for GF120918 was shifted to higher concentrations in KB 8-5-11 cells, which express high levels of *MDR1* P-glycoprotein (Figure 5). In this cell line, the EC_{50} values for GF120918 were ≈10-fold higher than in the KB 8-5 cells (Table 1). Conversely, cell content of the Tc complexes in KB 3-1 cells was not affected by GF120918 concentrations between 10^{-8} and 3×10^{-6} M (data not shown). As anticipated, methotrexate and *cis*-platin, chemotherapeutic agents that are not included in the multidrug resistance phenotype, had no effect on accumulation of any Tc complex in KB 8-5 or 8-5-11 cells at concentrations between 1 and 500 μM (data not shown).

MDR1 P-Glycoprotein Transport of Q Complexes in KB Cells. To further characterize transport of Q complexes mediated by *MDR1* P-glycoprotein, accumulation of Tc−Q58 and Tc−Q63 in KB 8-5 cells after 30 min of incubation was determined as a function of extracellular concentration of each radiopharmaceutical. At extracellular concentrations of Tc−Q58 between 10 and 333 pM, cell content of the Q complex was constant at 1.8 ± 0.2 fmol (mg of protein)$^{-1}$ $(nM_0)^{-1}$ ($n = 20$) and increased to a constant accumulation value of 31.5 ± 3.0 fmol (mg of protein)$^{-1}$ $(nM_0)^{-1}$ ($n = 20$) in the presence of a near maximal inhibitory concentration of GF120918 (300 nM). Using extracellular concentrations of Tc−Q63 between 25 and 280 pM, cell content of this radiopharmaceutical was constant at 10.1 ± 0.7 and 199 ± 12 fmol (mg of protein)$^{-1}$ $(nM_0)^{-1}$ ($n = 20$) in the absence or presence of 300 nM GF120918, respectively. Thus, no evidence of saturation of transport by *MDR1* P-glycoprotein was seen for either Q complex over the range of concentrations analyzed. A high capacity for transport of Tc−Sestamibi by *MDR1* P-glycoprotein has been reported previously over a much greater range of concentrations, with no saturation of transport kinetics observed between 7 pM and 10 μM (*27*).

Specificity of Q Complexes for MDR1 Compared with MDR3 P-Glycoprotein in Baculoviral Expression System

To further validate Tc−Q58 and Tc−Q63 as substrates for transport by *MDR1* P-glycoprotein and to determine if the Q complexes are substrates for *MDR3* P-glycoprotein, transport assays were performed in Sf9 cells infected with wild-type baculovirus or recombinant baculoviruses containing human *MDR1* or *MDR3*. Sf9 cells and cells infected with wild-type baculovirus do not express immunodetectable P-glycoprotein (Figure 6). P-glycoproteins are expressed in cells infected with either *MDR1*- or *MDR3*-containing baculoviruses. As seen in the Western blot, relative expression of *MDR1* P-glycoprotein was consistently greater than that of *MDR3* in the baculovirus system. Differences in expression of *MDR1* and *MDR3* P-glycoproteins also have been observed previously in yeast (*39*), mammalian cells (*40*), and in our own laboratory (V. V. Rao and D. Piwnica-Worms, unpublished data).

Table 1: Effect of MDR Modulators on Cellular Accumulation of Tc Complexes[a]

		Tc−Q63		Tc−Q58		Tc−Sestamibi	
cells	drug	EC_{50}	C_{max}	EC_{50}	C_{max}	EC_{50}	C_{max}
KB 8-5	cyclosporin A	3.0	344 ± 27	2.5	43.8 ± 1.0	1.3	332 ± 38
	verapamil	178	132 ± 8	354	46.8 ± 2.1	257	354 ± 17
	GF120918	0.034	291 ± 28	0.029	29.2 ± 0.5	0.031	280 ± 8
KB 8-5-11	GF120918	0.30	415 ± 86	0.23	43.2 ± 9.2	0.28	332 ± 18
MDR1 Sf9	GF120918	0.027	369 ± 13	0.070	91.8 ± 10.0	0.052	668 ± 17

[a] Pharmacological characterization (eq 1) of concentration−effect curves for drug-induced enhancement of Tc complexes in various cell lines. 30-min Tc complex accumulation in the presence or absence of drug was assayed at various concentrations (10^{-9} M to 5×10^{-4} M) (n = three to eight determinations each). Cellular accumulation of each complex is expressed as [fmol (mg of protein)$^{-1}$ $(nM_0)^{-1}$]. EC_{50}, half-maximal effective concentration [μM]. C_{max}, maximal cell content of Tc complex, ± SEM. EC_{50} values for each modulator in the indicated cell type did not differ significantly among the Tc complexes, except for GF120918 in the *MDR1* expressing Sf9 cells.

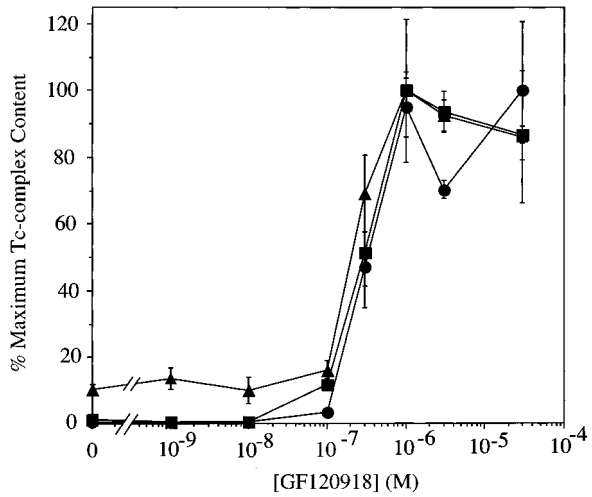

FIGURE 5: Effects of GF120918 on Tc complex cellular accumulation in highly drug-resistant cells. KB 8-5-11 cells were incubated for 30 min in buffer containing a different Tc complex (Tc−Q58, ▲; Tc−Q63, ■; Tc−Sestamibi, ●) and the indicated concentrations of GF120918. Accumulation of each Tc complex is plotted as the percent of maximal cellular content of each complex. Each point represents the mean of four determinations; bars represent ± SEM.

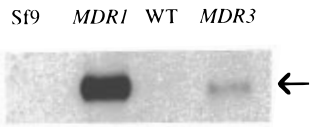

FIGURE 6: Expression of P-glycoprotein in Sf9 cells and Sf9 cells infected with recombinant *MDR1* baculovirus, wild-type virus, and recombinant *MDR3* baculovirus as determined by Western blots of membrane preparations with mAb C219. The arrow identifies 140 kDa.

Accumulation of Tc−Q58 and Tc−Q63 in the baculovirus system was quantified in monolayers of cells incubated in buffer with tracer amounts of each radiopharmaceutical for 30 min. Cell contents of Tc−Q58 and Tc−Q63 in cells infected with a wild-type baculovirus were 44.1 ± 5.1 and 524 ± 12 fmol (mg of protein)$^{-1}$ $(nM_0)^{-1}$ (n = 4), respectively. In cells expressing *MDR1* P-glycoprotein, accumulation of Tc−Q58 was decreased to 24.5 ± 3.9 fmol (mg of protein)$^{-1}$ $(nM_0)^{-1}$ (n = 16; $p < 0.01$ compared with wild-type baculovirus), while content of Tc−Q63 was reduced to 248 ± 14 fmol (mg of protein)$^{-1}$ $(nM_0)^{-1}$ (n = 8; $p < 0.001$). For both Tc complexes, expression of *MDR1* P-glycoprotein reduced accumulation of the respective Q complex by approximately half. In contrast, cell contents of Tc−Q58 and Tc−Q63 were not affected by expression of *MDR3* P-glycoprotein, resulting in values comparable to infection by wild-type virus [44.8 ± 1.7 (n = 16) and 598 ± 103 fmol (mg of protein)$^{-1}$ $(nM_0)^{-1}$ (n = 12) for Tc−Q58 and Tc−Q63, respectively].

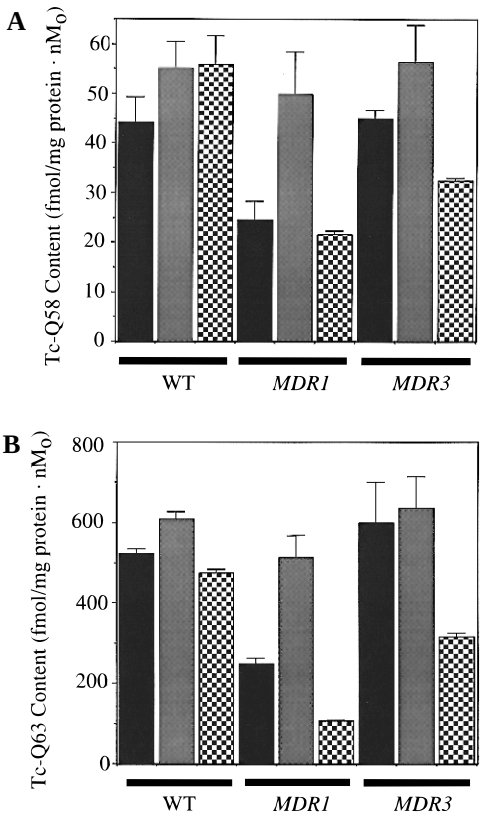

FIGURE 7: Effects of various drugs on accumulation of Tc complexes in Sf9 cells. Sf9 cells infected with wild-type virus (WT), recombinant virus with *MDR1* (*MDR1*), and recombinant virus with *MDR3* (*MDR3*) were used for transport assays 44−48 h after infection. Infected Sf9 cells were incubated for 30 min with Tc−Q58 (A) or Tc−Q63 (B) in buffer alone (black bars), 300 nM GF120918 (gray bars), or 200 μM cis-platin (checkerboard bars). Columns are the mean of 4−16 determinations; small bars represent + SEM. Note different scales for cellular accumulation of Tc−Q58 (A) or Tc−Q63 (B).

Effects of the MDR modulator GF120918 on accumulation of Q complexes in the baculovirus system also were determined. A maximal inhibitory dose of GF120918 (300 nM) was used on the basis of drug concentration−effect curves in the KB cells. In Sf9 cells expressing *MDR1* P-glycoprotein, GF120918 enhanced accumulation of each Tc complex to levels seen in cells infected with wild-type virus [49.8 ± 8.5 and 514 ± 54 fmol (mg of protein)$^{-1}$ $(nM_0)^{-1}$ (n = 4−16) for Tc−Q58 and Tc−Q63 in *MDR1* expressing cells, respectively; Figure 7]. In cells infected with wild-type or *MDR3*-containing baculoviruses, GF120918

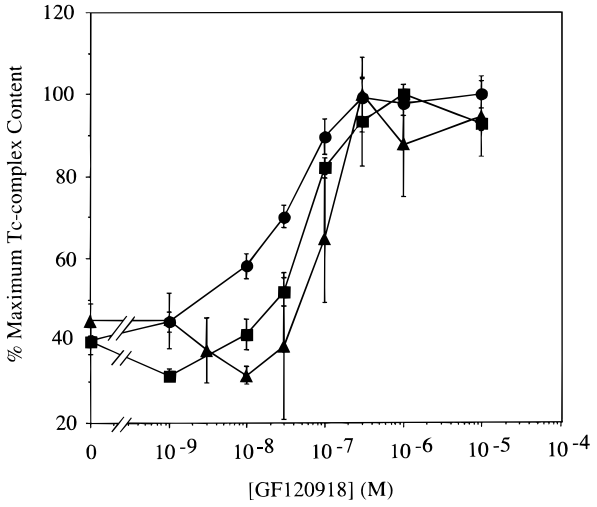

FIGURE 8: Effects of GF120918 on Tc complex cellular accumulation in Sf9 cells expressing *MDR1* P-glycoprotein. Sf9 cells were infected with recombinant baculovirus containing *MDR1* and assayed 44−48 h after infection. Cells were incubated for 30 min in buffer containing a different Tc complex (Tc−Q58, ▲; Tc−Q63, ■; Tc−Sestamibi, ●) and the indicated concentrations of GF120918. Data are presented as the percent of maximal accumulation of each Tc complex. Each point represents the mean of four to eight determinations; bars represent ± SEM.

did not significantly affect net cell content of either Q complex, except for Tc−Q63 in cells infected with wild-type viruses. As expected, high-dose *cis*-platin either did not change or decreased cell content of both Q complexes in all cells. Similar results were observed when cells were incubated with high doses of methotrexate (data not shown). The observed decrease in overall accumulation of the Q complexes by these chemotherapeutic drugs likely is caused by toxicity of the agents to cells. The effects of GF120918, methotrexate, and *cis*-platin on cellular content of Tc−Sestamibi in the baculovirus system were comparable to those observed with the Q complexes. GF120918 increased cellular content of Tc−Sestamibi only in cells expressing *MDR1* P-glycoprotein, while no effect on accumulation of this Tc complex was seen with methotrexate or *cis*-platin (data not shown).

A wide range of concentrations of GF120918 was used to determine the apparent potency of this modulator to enhance cell content of each Tc complex in host cells infected with viruses containing *MDR1* (Figure 8). Increased accumulation of each radiopharmaceutical was seen, consistent with inhibition of *MDR1* P-glycoprotein-mediated efflux of both Q complexes and Tc−Sestamibi. EC_{50} values for transport inhibition by GF120918 were ≤70 nM for all three Tc complexes (Table 1).

Functional Status of P-Glycoprotein at the Blood−Brain Barrier in vivo As Probed with Tc−Q58

Drug-transporting P-glycoproteins (*MDR1* in humans and *mdr1a* in mice) have an important physiologic function at the blood−brain barrier, limiting entry of many different amphipathic compounds into the central nervous system (*41*). To characterize the potential use of Q complexes as markers of the transport function and modulation of P-glycoprotein *in vivo*, we determined the biodistribution of Tc−Q58 in blood and brain tissue of FVB mice following intravenous injection of the tracer (Figure 9). To inhibit P-glycoprotein

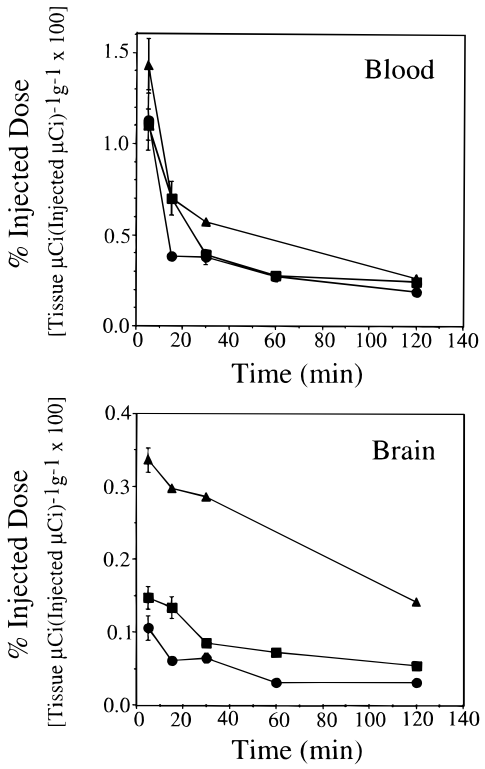

FIGURE 9: Pharmacokinetics of Tc−Q58 in blood and brain of FVB mice. Parental FVB mice were administered GF120918 (250 mg/kg, ■) or vehicle alone (●), and *mdr1a* (−/−) mice (▲) also received vehicle alone by oral gavage 4 h prior to intravenous bolus injection of ^{99m}Tc−Q58. Data are expressed as percent of injected dose of radioactivity per gram of tissue at the respective time point. For parental mice treated with vehicle alone or GF120918, data points represent the mean of three to four determinations; for *mdr1a* (−/−) mice, data points represent the mean of three determinations for the 5 min time point and two determinations for all other times. Bars represent ± SEM for $n > 2$ when larger than the symbol.

at the blood−brain barrier, GF120918 (250 mg/kg) was administered by oral gavage to FVB mice 4 h prior to injection of Tc−Q58; this dosing regimen produces serum levels of drug that maximally inhibit P-glycoprotein (*32*). Blood pharmacokinetics of Tc−Q58 were not significantly changed following administration of GF120918 [area-under-the-curve (AUC_{5-120}) = 36.8 ± 5.0 vs 42.9 ± 5.4 μCi (injected μCi)$^{-1}$ (g of tissue)$^{-1}$ × 100 ·min in the absence and presence of GF120918, respectively, $p > 0.4$]. Penetration of Tc−Q58 into brain tissue of parental FVB mice was very limited, with an AUC_{5-120} of 5.1 ± 0.5 μCi (injected μCi)$^{-1}$ (g of tissue)$^{-1}$ × 100·min ($n = 17$), demonstrating exclusion of the tracer relative to blood. By comparison, in mice treated with GF120918, the AUC_{5-120} for Tc−Q58 in brain tissue increased to 9.2 ± 0.9 μCi (injected μCi)$^{-1}$ (g of tissue)$^{-1}$ × 100·min ($n = 18$), a value 180% above control ($p < 0.001$). Thus, increased accumulation and retention of Tc−Q58 in brain tissue following treatment with GF120918 were consistent with expectations for inhibition of P-glycoprotein in the capillary endothelium and could not be attributed to differences in pharmacokinetics of Tc−Q58 in blood.

Although mice have two isoforms of P-glycoprotein that confer multidrug resistance, only *mdr1a* is expressed in endothelial cells of capillaries at the blood−brain barrier (*41*). Thus, *mdr1a* (−/−) mice have no drug-transporting P-glycoprotein at the blood−brain barrier. To further dem-

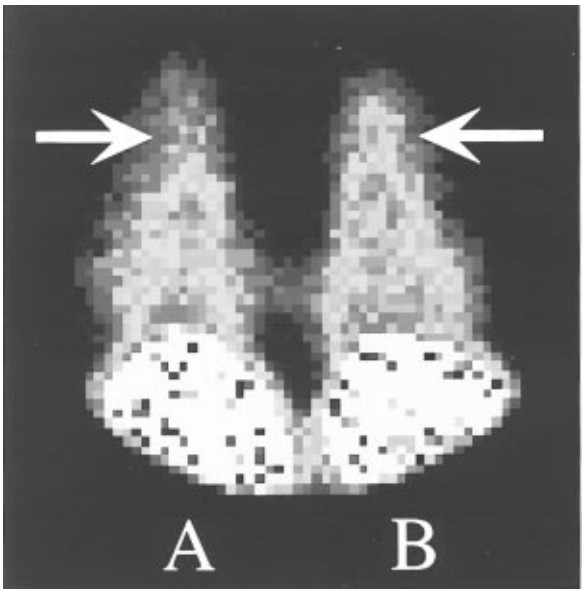

FIGURE 10: Scintigraphic image of accumulation of ^{99m}Tc−Q58 in brains of FVB parental and *mdr1a* (−/−) mice. Following injection of mice with an intravenous bolus of ^{99m}Tc−Q58, posterior images of the thorax and head of each animal were obtained with a gamma scintillation camera. Representative planar images of parental (A) and *mdr1a* (−/−) (B) mice obtained 5 min postinjection are shown. *Arrows* indicate gamma emissions from brain; note masked radioactivity in liver parenchyma.

onstrate that drug-transporting P-glycoprotein at the blood−brain barrier excludes Tc−Q58 from brain, we analyzed initial uptake and retention of the tracer in *mdr1a* (−/−) mice (Figure 9). In comparison with parental FVB mice, *mdr1a* (−/−) mice showed ≈320% more Tc−Q58 in brain parenchyma 5 min after injection of the Q complex. Additionally, the AUC_{5-120} of Tc−Q58 in brain significantly increased to 26.8 ± 3.2 μCi (injected μCi)$^{-1}$ (g of tissue)$^{-1}$ × 100·min (n = 9), a value 530% greater than that of parental FVB mice ($p \ll 0.001$). By contrast, blood retention of ^{99m}Tc−Q58 in *mdr1a* (−/−) mice was 57.7 ± 5.6 μCi (injected μCi)$^{-1}$ (g of tissue)$^{-1}$ × 100·min, only 160% of FVB control ($p = 0.01$). Net penetration of Tc−Q58 into brain tissue of *mdr1a* (−/−) mice also was 290% of that found in FVB mice treated with GF120918 ($p \ll 0.001$). Because blood flow to the brain does not differ between the parental and *mdr1a* (−/−) mice (*42*), the observed enhancement in penetration and retention of Tc−Q58 in brains of *mdr1a* (−/−) mice cannot be attributed to differences in cerebral perfusion. These data support the hypothesis that Tc−Q58 is a substrate for drug-transporting P-glycoproteins and can be used as a marker of function and inhibition of these proteins *in vivo*.

To further evaluate potential use of these Q complexes as probes of P-glycoprotein at the blood−brain barrier *in vivo*, we exploited the gamma-emission spectrum of ^{99m}Tc to produce scintigraphic images of brains of mice injected with ^{99m}Tc−Q58. A representative image of brain uptake of ^{99m}Tc−Q58 at 5 min after injection in parental and *mdr1a* (−/−) mice is shown in Figure 10. Increased accumulation of Tc−Q58 is evident within the brain of the *mdr1a* (−/−) mouse as compared with the parental mouse. Gamma emissions from Tc−Q58 in brain were 16% greater in *mdr1a* (−/−) mice compared to control (n = 2), as determined by counts per minute in regions of interest delineated over heads of mice on the scintigraphic images.

DISCUSSION

Although reversal of MDR mediated by P-glycoprotein has been achieved *in vitro* with a variety of pharmacological agents, use of some modulators *in vivo* has been limited by side effects, including neurological toxicities. To efficiently determine the efficacy and toxicity of new second- and third-generation modulators in patients, surrogate markers of the functional status of P-glycoprotein *in vivo* are needed. One potential marker of P-glycoprotein *in vivo* is ^{99m}Tc−Sestamibi, a gamma-emitting radiopharmaceutical originally developed for heart imaging, which has been validated as a substrate for *MDR1* P-glycoprotein (*21*). Utilizing ^{99m}Tc−Sestamibi for imaging, detection of the transport function of P-glycoprotein in normal tissues (liver and kidneys) (*43*) and tumors (*44*) and modulation by PSC 833 have been reported in patients (*43*, *45*). However, radioprobes specifically designed to interact with *MDR1* P-glycoprotein might improve detection of functional expression of this protein and quantification of successful inhibition following treatment with a modulator *in vivo*.

$N_2O_2P_2$−technetium(III) complexes (Q complexes) are monocationic, hydrophobic mixed ligand compounds with the general formula $[Tc(III)LY_2]^+$, where L is a tetradentate, dianionic ligand and Y is a monodentate tertiary phosphine (*16*). The technetium core of these Q complexes is quite stable in the Tc(III) state; reduction to Tc(II) does not occur at potentials found in biological systems (*17*). Additionally, these agents are generally not metabolized *in vivo*. The biochemical properties of these complexes are altered by modifying the substituents on the Schiff base and the tertiary phosphine. We recently completed a systematic screening of 38 different Q complexes as potential substrates for transport by P-glycoprotein and identified Tc−Q58 and Tc−Q63 as candidate radiopharmaceuticals for further investigation as probes of the transport activity of *MDR1* P-glycoprotein (*18*).

In the current study, we have extended these preliminary observations by characterizing the biochemical pharmacology of Tc−Q58 and Tc−Q63 transport in mammalian cell lines expressing differing amounts of P-glycoprotein and a recombinant baculovirus system specifically overexpressing *MDR1* P-glycoprotein. Data from both systems support the hypothesis that Tc−Q58 and Tc−Q63 are transport substrates recognized by *MDR1*, but not *MDR3* P-glycoprotein. Specifically, (1) net cellular accumulation of both Q complexes was inverse to expression of P-glycoprotein in KB cells; (2) known modulators of P-glycoprotein increased cell contents of Q complexes in multidrug-resistant cells to levels observed in drug-sensitive cells; (3) EC_{50} values for modulators were consistent with known values for half-maximal inhibition of *MDR1* P-glycoprotein and were comparable for the Q complexes and Tc−Sestamibi (*27*, *32*); (4) cytotoxic agents not included in the multidrug-resistance phenotype did not alter accumulation of Tc−Q58 or Tc−Q63 in cells; and (5) cell content of both Q complexes was decreased in Sf9 cells expressing recombinant human *MDR1* P-glycoprotein, but not the homologous *MDR3* protein, as compared with control infection by wild-type baculovirus.

While the detailed biochemical mechanism of action of P-glycoprotein remains under active investigation, recent studies have focused attention on the flippase model for *MDR1* P-glycoprotein (*3*, *40*, *46*). The murine *mdr2*

protein (homologous to human *MDR3*) functions as a flippase of phosphatidylcholine in membranes, and studies of the LmrA protein in *Lactococcoccus lactis* also support a membrane flippase model (*47*, *48*). In epithelial cells transfected with human *MDR1*, a broad range of short acyl chain analogues of membrane lipids were translocated across the plasma membrane, while cells expressing *MDR3* only translocated a short-chain analogue of phosphatidylcholine (*40*). Transport of membrane lipids with long acyl chains was not analyzed, although the murine *mdr1a* P-glycoprotein (homologous to human *MDR1*) does not compensate for the defect in transport of long acyl chain phosphatidylcholine in *mdr2* knock-out mice (*49*). These studies would suggest that the acyl chain length at the *sn*-2 position of phospholipids is a key determinant of recognition by *MDR1* versus *MDR3*. By contrast, a recent study with fluorescent analogues and radiolabeled phospholipids supports the hypothesis that human *MDR1* P-glycoprotein may indeed be a flippase of long-chain phosphatidylcholine and phosphatidylethanolamine (*23*). Potentially, our data suggest that Q complexes may serve as a general scaffold for simulating phospholipids and determining structure−activity relationships for recognition as substrates for transport by *MDR1* and differentiation between *MDR1* and *MDR3* P-glycoproteins. We speculate that the delocalized charge of the Q complexes mimics the polar head group of phospholipids and that substituents of the phosphines and Schiff base could be systematically modified to simulate acyl chains of phospholipids. We are in the process of developing such compounds for structure−activity studies of recognition determinants for *MDR1* and *MDR3* P-glycoproteins.

Multidrug resistance in tumors also can be due to overexpression of MRP, another member of the ABC transporter family (*7*). MRP typically transports compounds that are amphipathic and anionic, such as leukotriene C_4, or compounds which have been conjugated to glutathione (*50*, *51*). However, recent studies have shown that natural product cytotoxic agents which are neutral or cationic in character also can be transported by MRP (*52*). While further studies are underway, even if Tc−Q58 and Tc−Q63 are substrates for MRP, use of modulators that are specific for *MDR1* P-glycoprotein, such as GF120918 (*53*), should differentiate transport mediated by these two ABC transporters *in vitro* and *in vivo*.

MDR1 P-glycoprotein is expressed in capillary endothelial cells in the brain where the protein is a major component of the blood−brain barrier (*14*). *mdr1a* (−/−) mice are an excellent model for investigating the role of P-glycoprotein in maintaining the blood−brain barrier, because *mdr1b*, the other isoform of P-glycoprotein associated with transport of chemotherapeutic drugs in mice, is not expressed at this site. Recently, mice deficient in both *mdr1a* and *mdr1b* [*mdr1a/1b* (−/−)] also have been generated, and these animals showed no significant differences in accumulation of digoxin within brain parenchyma compared with *mdr1a* (−/−) mice, further demonstrating that only *mdr1a* is important for P-glycoprotein-mediated function at the blood−brain barrier in mice (*54*). Our biodistribution and imaging data now show that function and modulation of P-glycoprotein at the blood−brain barrier can be readily detected with tracer concentrations of Tc−Q58. Note that compared to FVB control, increased accumulation of tracer in *mdr1a* (−/−) mice relative to FVB mice treated with GF120918 likely reflected differences between complete absence of drug-transporting P-glycoprotein in the former animals versus pharmacological inhibition of *mdr1a* P-glycoprotein in the latter. Using the gamma-emissions of ^{99m}Tc, we were also able to detect by scintigraphy greater net uptake of Tc−Q58 in *mdr1a*(−/−) mice compared with the parental strain *in vivo*. However, quantitative differences in distribution and retention of Tc−Q58 in brain between the parental and *mdr1a* (−/−) mice were less as measured on scintigraphic images than in tissues from biodistribution experiments. This discrepancy in part likely reflects spatial limitations of imaging mice with a conventional gamma scintillation camera designed for humans; gamma-emissions from ^{99m}Tc−Q58 within brain parenchyma cannot be distinguished from scattered radioactivity present in overlying soft tissues using a region-of-interest cursor placed over the head on a planar scintigraphic image. Nevertheless, increased accumulation of Tc−Q58 in brain of the *mdr1a* (−/−) mouse was readily apparent on the planar scintigraphic images, and application of tomographic techniques (SPECT) may further enhance detectability.

We envision that the gamma-emissions of ^{99m}Tc−Q58 (or potentially ^{99m}Tc−Q63) could be used to monitor inhibition of P-glycoprotein at the blood−brain barrier noninvasively, with functional imaging performed before and after treatment of patients with a modulator of *MDR1* P-glycoprotein. By using Tc−Q58 as a surrogate marker of transport function of *MDR1* P-glycoprotein, imaging with this Q complex potentially could be used to predict neurotoxicity associated with modulator therapy in combination with cytotoxic drugs. In addition, Tc−Q58 also could be used for detection of functional P-glycoprotein in tumors and effective inhibition of this transporter following treatment with a modulator (*43*, *45*). By coordinating the administration of chemotherapeutic drugs that are substrates for *MDR1* P-glycoprotein with the time of maximum inhibition from a modulator, therapy could be optimized. Thus, pharmacokinetic mapping of P-glycoprotein with Tc complexes potentially can be used to improve therapy for patients treated with cytotoxic drugs in the MDR phenotype.

In conclusion, we have shown that Tc−Q58 and Tc−Q63 are both transport substrates for *MDR1*, but not *MDR3* P-glycoprotein. Picomolar concentrations of both complexes are recognized and transported by *MDR1* P-glycoprotein, making them sensitive markers for the functional activity of this membrane protein. While these compounds are structurally analogous and show similar transport profiles for *MDR1* P-glycoprotein, the two radiopharmaceuticals behave quite differently in assays of cells that do not express *MDR1*. Tc−Q63 shows significant apparent adsorption to lipids, while binding to lipid compartments in cells appears minimal for Tc−Q58. Thus, Tc−Q58 and Tc−Q63 are novel probes of *MDR1* P-glycoprotein that can be used together to further investigate the transport mechanisms of this protein. By exploiting the gamma-emission spectrum of ^{99m}Tc, these Q complexes also can be used for noninvasive imaging of *MDR1* P-glycoprotein transport function and modulation *in vivo*.

ACKNOWLEDGMENT

We thank Mary Marmion and Elizabeth Webb, Mallinckrodt, Inc., for synthesis of the radiolabeled ^{99m}Tc−Q com-

plexes; Michael Gottesman, National Institutes of Health, for the KB cell lines; James Croop, Dana Farber Cancer Institute, for the baculoviral constructs; and DeLynn Barrie, Division of Nuclear Medicine, for technical assistance.

REFERENCES

1. Gottesman, M. M., and Pastan, I. (1988) *J. Biol. Chem. 263*, 12163−12166.
2. Endicott, J. A., and Ling, V. (1989) *Annu. Rev. Biochem. 58*, 137−171.
3. Gottesman, M. M., and Pastan, I. (1993) *Annu. Rev. Biochem. 62*, 385−427.
4. Gros, P., Ben Neriah, Y., Croop, J. M., and Housman, D. E. (1986) *Nature 323*, 728−731.
5. Shen, D. W., Fojo, A., Chin, J. E., Roninson, I. B., Richert, N., Pastan, I., and Gottesman, M. M. (1986) *Science 232*, 643−645.
6. Ford, J. M., and Hait, W. N. (1990) *Pharmacol. Rev. 42*, 155−199.
7. Cole, S. P. C., Bhardwaj, G., Gerlach, J. H., Mackie, J. E., Grant, C. E., Almquist, K. C., Stewart, A. J., Kurz, E. U., Duncan, A. M. V., and Deeley, R. G. (1992) *Science 258*, 1650−1654.
8. Chan, H. S. L., Haddad, G., Thorner, P. S., DeBoer, G., Lin, Y. P., Ondrusek, N., Yeger, H., and Ling, V. (1991) *N. Engl. J. Med. 325*, 1608−1614.
9. Baldini, N., Scotlandi, K., Barbanti-Brodano, G., Manara, M., Maurici, D., Bacci, G., Bertoni, F., Picci, P., Sottili, S., Campanacci, M., and Serra, M. (1995) *N. Engl. J. Med. 333*, 1380−1385.
10. Linn, S., Giaccone, G., van Diest, P., Blokhuis, W., van der Valk, P., van Kalken, C., Kuiper, C., Pinedo, H., and Baak, J. (1995) *Ann. Oncol. 6*, 679−685.
11. Norris, M., Bordow, S., Marshall, G., Haber, P., Cohn, S., and Haber, M. (1996) *N. Engl. J. Med. 334*, 231−238.
12. Trock, B., Leonessa, F., and Clarke, R. (1997) *J. Natl. Cancer Inst. 89*, 917−931.
13. Cordon-Cardo, C., O'Brien, J. P., Boccia, J., Casals, D., Bertino, J. R., and Melamed, M. R. (1990) *J. Histochem. Cytochem. 38*, 1277−1287.
14. Schinkel, A., Smit, J., van Tellingen, O., Beijnen, J., Wagenaar, E., van Deemter, L., Mol, C., van der Valk, M., Robanus-Maandag, E., te Riele, H., Berns, A., and Borst, P. (1994) *Cell 77*, 491−502.
15. Boote, D., Dennis, I., Twentyman, P., Osborne, R., Laburte, C., Hensel, S., Smyth, J., Brampton, M., and Bleehan, N. (1996) *J. Clin. Oncol. 14*, 610−618.
16. Jurisson, S. S., Dancey, K., McPartlin, M., Tasker, P. A., and Deutsch, E. (1984) *Inorg. Chem. 23*, 4743−4749.
17. Deutsch, E., Vanderheyden, J.-L., Gerundini, P., Libson, K., Hirth, W., Colombo, F., Savi, A., and Fazio, F. (1987) *J. Nucl. Med. 28*, 1870−1880.
18. Crankshaw, C., Marmion, M., Luker, G., Rao, V., Dahlheimer, J., Burleigh, B., Webb, E., Deutsch, K., and Piwnica-Worms, D. (1997) *J. Nucl. Med.* (in press).
19. Chiu, M. L., Kronauge, J. F., and Piwnica-Worms, D. (1990) *J. Nucl. Med. 31*, 1646−1653.
20. Piwnica-Worms, D., Jacob, R., Horres, C. R., and Lieberman, M. (1983) *J. Gen. Physiol. 81*, 731−748.
21. Piwnica-Worms, D., Chiu, M. L., Budding, M., Kronauge, J. F., Kramer, R. A., and Croop, J. M. (1993) *Cancer Res. 53*, 977−984.
22. Akiyama, S. I., Fojo, A., Hanover, J. A., Pastan, I., and Gottesman, M. M. (1985) *Somatic Cell Mol. Genet. 11*, 117−126.
23. Bosch, I., Dunussi-Joannopoulos, K., Wu, R.-L., Furlong, S., and Croop, J. (1997) *Biochemistry 36*, 5685−5694.
24. Rao, V. V., Chiu, M. L., Kronauge, J. F., and Piwnica-Worms, D. (1994) *J. Nucl. Med. 35*, 510−515.
25. Piwnica-Worms, H. (1990) *Curr. Protocols*, 16.8−16.11.
26. Summers, M. D., and Smith, G. E. (1987) *Texas Agric. Exp. Stn. Bull. No. 1555*.
27. Piwnica-Worms, D., Rao, V., Kronauge, J., and Croop, J. (1995) *Biochemistry 34*, 12210−12220.
28. Piwnica-Worms, D., Kronauge, J. F., and Chiu, M. L. (1990) *Circulation 82*, 1826−1838.
29. Lowry, O. H., Rosenbrough, W. F., Farr, A. L., and Randall, R. J. (1951) *J. Biol. Chem. 193*, 265−275.
30. Lamson, M. L., Kirscher, A. S., Hotte, C. E., Lipsitz, E. L., and Ice, R. D. (1975) *J. Nucl. Med. 16*, 639−641.
31. Herman, L. W., Sharma, V., Kronauge, J. F., Barbarics, E., Herman, L. A., and Piwnica-Worms, D. (1995) *J. Med. Chem. 38*, 2955−2963.
32. Hyafil, F., Vergely, C., Du Vignaud, P., and Grand-Perret, T. (1993) *Cancer Res. 53*, 4595−602.
33. Sharma, V., Crankshaw, C., and Piwnica-Worms, D. (1996) *J. Med. Chem. 39*, 3483−3490.
34. Ritchie, R. J. (1984) *Prog. Biophys. Mol. Biol. 43*, 1−32.
35. Piwnica-Worms, D., Kronauge, J. F., and Chiu, M. L. (1991) *J. Nucl. Med. 32*, 1992−1999.
36. Chernoff, D. M., Strichartz, G. R., and Piwnica-Worms, D. (1993) *Biochim. Biophys. Acta 1147*, 262−266.
37. Winegar, D., Salisbury, J., Sundseth, S., and Hawke, R. (1996) *J. Lipid Res. 37*, 179−191.
38. Hemenway, C., and Heitman, J. (1996) *J. Biol. Chem. 271*, 18527−18534.
39. Ruetz, S., and Gros, P. (1994) *J. Biol. Chem. 269*, 12277−12284.
40. van Helvoort, A., Smith, A. J., Sprong, H., Fritzsche, I., Schinkel, A. H., Borst, P., and van Meer, G. (1996) *Cell 87*, 507−517.
41. Schinkel, A. H., Mol, C. A. A. M., Wagenaar, E., van Deemter, L., Smit, J. J. M., and Borst, P. (1995) *Eur. J. Cancer 31A*, 1295−1298.
42. Franssen, E., Hendrikse, N., Elsinga, P., Fluks, E., Schinkel, A., van der Graaf, W., van Loenen-Weemaes, A., de Vries, E., and Vaalburg, W. (1996) *J. Nucl. Med. 37*, 355P.
43. Luker, G. D., Fracasso, P. M., Dobkin, J., and Piwnica-Worms, D. (1997) *J. Nucl. Med. 38*, 369−372.
44. Del Vecchio, S., Ciarmiello, A., Potena, M. I., Carriero, M. V., Mainolfi, C., Botti, G., Thomas, R., Cerra, M., D'Aiuto, G., Tsuruo, T., and Salvatore, M. (1997) *Eur. J. Nucl. Med. 24*, 150−159.
45. Chen, C., Meadows, B., Regis, J., Kalafsky, G., Fojo, T., Carrasquillo, J., and Bates, S. (1997) *Clin. Cancer Res. 3*, 545−552.
46. Higgins, C. F., and Gottesman, M. M. (1992) *Trends Biochem. Sci. 17*, 18−21.
47. Ruetz, S., and Gros, P. (1994) *Cell 77*, 1071−1081.
48. van Veen, H., Venema, K., Bolhuis, H., Oussenko, I., Kok, J., Poolman, B., Driessen, A., and Konings, W. (1996) *Proc. Natl. Acad. Sci. U.S.A. 93*, 10668−10672.
49. Smit, J., Schinkel, A., Oude Elferink, R., Groen, A., Wagenaar, E., van Deemter, L., Mol, C., Ottenhoff, R., van der Lugt, N., van Roon, M., van der Valk, M., Berns, A., and Borst, P. (1993) *Cell 75*, 451−462.
50. Evers, R., Zaman, J., van Deemter, L., Jansen, H., Calafat, J., Oomen, L., Oude Elferink, R., Borst, P., and Schinkel, A. H. (1996) *J. Clin. Invest. 97*, 1211−1218.
51. Ruetz, S., Brault, M., Kast, C., Hemenway, C., Heitman, J., Grant, C., Cole, S., Deeley, R., and Gros, P. (1996) *J. Biol. Chem. 271*, 4154−4160.
52. Paul, S., Breuninger, L., and Kruh, G. (1996) *Biochemistry 35*, 14003−14011.
53. Germann, U., Ford, P., Schlakhter, D., Mason, V., and Harding, M. (1997) *Anticancer Drugs 8*, 141−155.
54. Schinkel, A., Mayer, U., Wagenaar, E., Mol, C., van Deemer, L., Smit, J., van der Valk, M., Voordouw, A., Spits, H., van Tellingen, O., Zijlmans, J., Fibbe, W., and Borst, P. (1997) *Proc. Natl. Acad. Sci. U.S.A. 94*, 4028−4033.

BI971931Z